

# Nb<sub>3</sub>Sn FILMS DEPOSITIONS FROM TARGETS SYNTHESIZED VIA LIQUID TIN DIFFUSION

M. Zanierato<sup>†</sup>, O. Azzolini, E. Chyhyrynets, V. Garcia Diaz, G. Keppel, F. Stivanello, C. Pira,  
 Legnaro National Laboratories (LNL) - Istituto Nazionale di Fisica Nucleare (INFN), Legnaro, Italy

## Abstract

The deposition of Nb<sub>3</sub>Sn on copper cavities is interesting for the higher thermal conductivity of copper compared to common Nb substrates. The better heat exchange would allow the use of cryocoolers reducing cryogenic costs and the risk of thermal quench [1]. Magnetron sputtering technology allows the deposition of Nb<sub>3</sub>Sn on substrates different than Nb, however the coating of substrates with complex geometry (such as elliptical cavities) may require targets with non-planar shape, difficult to realize with classic powder sintering techniques. In this work, the possibility of using the Liquid Tin Diffusion (LTD) technique to produce sputtering targets is explored. The LTD technique is a wire fabrication technology, already developed in the past at LNL for SRF applications [2], that allows the deposition of very thick and uniform coating on Nb substrates even with complex geometry [3]. Improvements in LTD process, proof of concept of a single use LTD target production, and characterization of the Nb<sub>3</sub>Sn film coated by DC magnetron sputtering with these innovative targets are reported in this work.

## INTRODUCTION

The thin film technology deposition of Nb<sub>3</sub>Sn represents an interesting perspective for superconducting radio frequency (SRF) applications. Nb<sub>3</sub>Sn shows potential limits, as critical temperature and theoretical accelerating gradient, that are higher with respect to Nb. The Nb<sub>3</sub>Sn thin films on Nb bulk cavities produced by Vapor Tin Diffusion (VTD) show excellent performances, but there is a strong interest in growing Nb<sub>3</sub>Sn on a Cu substrate, because of its higher thermal conductivity, by PVD techniques [1].

The features required for the cylindrical cathode cooling related to the fragility of the material, make the classic sintering from powders difficult to implement.

One possible solution is the production of the targets by growing thick films of Nb<sub>3</sub>Sn on a niobium substrate with Liquid Tin Diffusion (LTD) technique [3].

Along the years, different coating methods for Nb<sub>3</sub>Sn have been developed and in particular, LTD has been deeply studied at LNL from 2005 to 2009 [2]. The LTD allows the formation of thick films on niobium substrates by direct immersion in molten tin. The films deposited with DC magnetron sputtering are analysed and the characteristics are correlated with the synthesis process via LTD.

The LTD technique allows the coating on substrates with complex geometry. The synthesis of cylindrical targets for 6 GHz and 1.3 GHz cavities at industrial level is relatively easy to scale.

## EXPERIMENTALS

The material under study is Nb<sub>3</sub>Sn synthesised on bulk Nb substrate. Two types of samples are studied: 37 small Nb bulk samples (30x15x3 mm) and 5 one-inch planar targets 3 mm thick. The niobium substrates are subjected to ultrasonic bath and subsequent BCP (Buffer Chemical Polishing) HF: HNO<sub>3</sub>: H<sub>3</sub>PO<sub>4</sub> in a 1:1:2 ratio from five to ten minutes. The substrates prepared for pre-nucleation are subsequently anodized at 20 V for one minute in NaOH solution to form a 70 nm Nb<sub>2</sub>O<sub>3</sub> layer. For each run, 2 samples at a time have been used: one anodized and one just polished with BCP to evaluate possible change in the film growth.

The LTD system consists of an ultra-high vacuum pumping system, a linear manipulator, a furnace used for heating the crucible containing the tin, a furnace used for annealing of the samples, and a water jacket. The main chamber is made of Inconel. The samples are fixed to the manipulator by niobium wires. The system is heated and evacuated to a base pressure of 10<sup>-8</sup> mbar. The dipping process is divided into various steps as described in Fig. 1 and Fig. 2. The total protocol is summarized below [4].

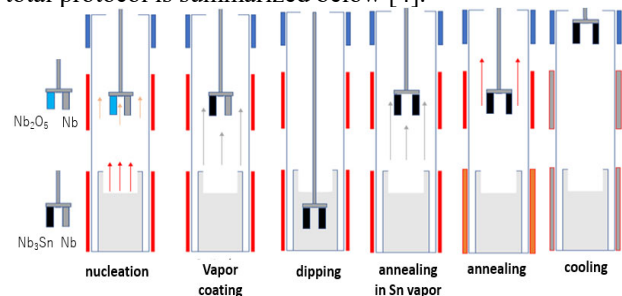


Figure 1: Samples position in the chamber in the dipping “hybrid” process with nucleation.

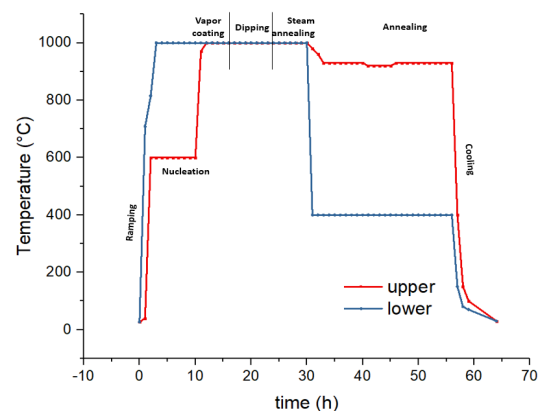


Figure 2: Temperature profiles of furnaces in the “hybrid” process with nucleation step for targets synthesis.

**Ramping:** the lower furnace is switched on to obtain degassing of the crucible in the bottom of the chamber, an hour later the upper furnace is switched on.

**Pre-Nucleation:** the substrates are located at the centre of the chamber in the annealing zone and remain there for 3 to 9 h at 600°C.

**Coating:** the upper furnace increases the temperature of the system to 1000°C and remains stable from 2 to 9 h.

**Dipping:** The substrates are immersed in the liquid tin crucible at 1000°C from 0.5 to 7 h by means of the manipulator.

**Steam annealing:** the samples brought back to the centre of the chamber are heated from 7.5 to 77 h in the presence of the tin vapours of the crucible at 1000°C.

**Annealing:** the lower furnace decreases in temperature blocking the tin landing on the surface of the samples allowing annealing from 15 to 84 h. The temperature of upper furnace should be near 1000°C.

**Cooling:** the samples are brought to the upper area of the water jacket to fix the phase.

### DC Magnetron Sputtering System

The DC Magnetron Sputtering system consists of an ultra-high vacuum pumping system, a 1-inch magnetron for housing the target obtained via LTD and a heatable sample holder. The system is heated to 750°C and evacuated to a base pressure of 10<sup>-6</sup> mbar. The post process annealing can be performed to increase A15 phase of the deposited film.

## RESULTS AND DISCUSSION

During the optimization process of the LTD technique, the following parameters were investigated: the influence of Nb anodization, the dipping time and the annealing time in the presence and absence of tin vapours.

The morphological and structural characterization allow to understand the quality of the film obtained.

Process	Sample	Nucleation Step	Coating Step	Dipping	Steam Annealing	Annealing
		T(°C) t(h)	T(°C) t(h)	T(°C) t(h)	T(°C) t(h)	T(°C) t(h)
P1	C1-C2	600	1000	1000	1000	1000
		2	2	3	6	15
P2	C3	/	/	1000 3	1000 21	/
P3	C4	/	/	1000 3	/	970 19
P4	C5	/	/	1000 3	1000 6	1000 15
P5	T1-T2	600	600	1000	1000	990
		9	9	5	36	60

Figure 3: Parameters used in Liquid Tin Diffusion process, C2 and T2 anodized samples.

### Sample Pretreatment

The great constraints found in old processes without Nb anodization are the formation of percolating paths inside the material with consequent incorporation of tin on the surface and small sintering of the grains [3]. By evaluating the liquidus curve in the Nb<sub>3</sub>Sn phase diagram under dipping conditions (Sn > 25% due to immersion in molten Sn), it is observed that a fraction of niobium can be solubilized in the bath.

From the SEM micrographs of the section of the films without anodization, Fig. 4 (D) process P1 described in Fig. 3, it is possible to observe the formation of percolation paths inside the film which determine a high porosity. For the realization of a target this would lead to a greater erosion of the film and inhomogeneity of the composition.

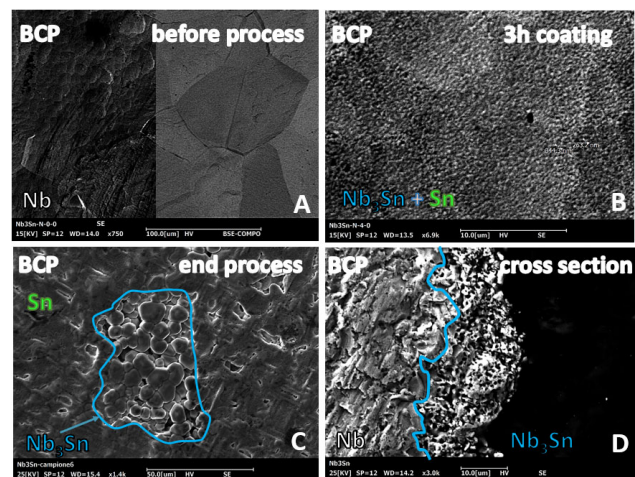


Figure 4: SEM micrographs of the sample treated only with BCP before the process (A), in the coating phase (B), at the complete process (C) with relative cross section (D).

The samples even after BCP Fig. 4 (A) exhibit approximately 6 nm of Nb<sub>2</sub>O<sub>5</sub> which promotes A15 crystallite formation. From the analysis of the micrographs in Fig 4 (B) it is possible to observe a degree of coverage of 93 % with crystallites having an average size greater than 250 nm. The EDS analysis confirms the presence of Sn from 17-30% in localized areas indicating a sporadic uncontrolled nucleation.

In the micrograph Fig. 4 (C) we observe the presence of residual Sn which partially covers the surface. In localized points, grains of Nb<sub>3</sub>Sn (25-30% Sn) of about 10 microns are present, excess tin is often found in grain boundaries.

In the cross section (D) it is possible to observe the residual porosity of the film.

The samples subjected to the anodizing treatment, as in Fig 5 (A), are treated to favour nucleation at 600°C, the coating step allows a growth of the Nb<sub>3</sub>Sn crystallites before the dipping step as shown in Fig 5 (B), relative to P1 process described in Fig.3. The growth occurs in the coating step and allows a first coating of the sample surface similarly to VTD. From the analysis of the micrographs in Fig. 5 (B) it is possible to observe a coverage of 96 % with crystallites having an average size greater than 250 nm. The process is conducted without SnCl<sub>2</sub> nucleating agent. The EDS analysis provides Sn concentration of 24-25% in large areas indicating a controlled nucleation. The presence of A15 film before dipping renders the substrate insoluble, limiting the formation of percolation paths.

The anodization of the substrate has a beneficial effect on the whole process, in fact in Fig. 5 (C) Nb<sub>3</sub>Sn crystallites are observed with correct stoichiometric composition and larger than 8 microns. The diffractometric analysis confirms the A15 phase and agrees with the EDS results.

The cross section of the film in Fig. 5 (D) shows a higher density when compared to the previous film (Fig. 4 D). The desired mean stoichiometry is maintained along the film.

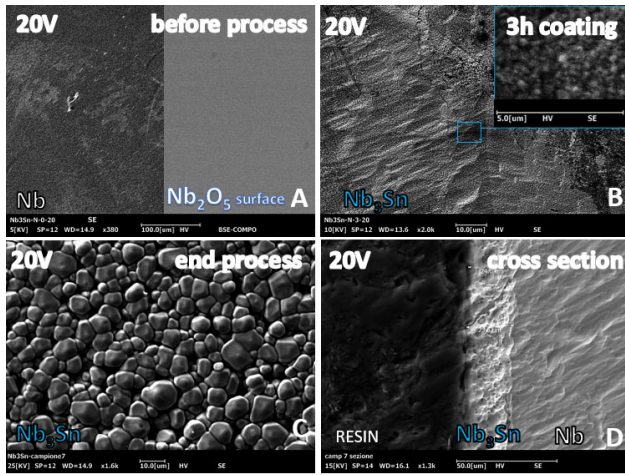


Figure 5: SEM micrographs of the anodized sample before the process (A), in the coating phase (B), at the complete process (C) with relative cross section (D).

### Dipping Time

The liquid phase diffusion processes are notoriously faster due to the higher diffusion coefficient and the establishment of new mechanisms at the grain boundaries. In the case of thick liquid, capillary pressure could also play an important role. An increase in thickness is observed by varying the dipping time.

To maintain the correct stoichiometry in thick films it is necessary to extend the annealing times. In Fig. 6 the thicknesses obtained by increasing the dipping step time in the hybrid process are plotted. Using the law of Fick, it is possible to obtain Eq. (1) for non-anodize samples and Eq. (2) for anodized samples with which it is possible to calculate the thickness obtained as a function of the dipping time.

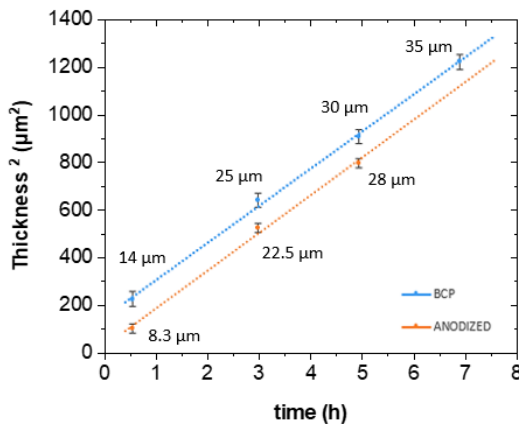


Figure 6: Graph of the thickness as a function of the dipping time for the anodized (orange) and non-anodized (blue) sample.

$$x_{BCP}^2 = 156.7 t + 129.5 \quad (1)$$

$$x_{anodized}^2 = 159.6 t + 0.9 \quad (2)$$

Where  $x$  is the thickness expressed in  $\mu\text{m}^2$  and  $t$  the time expressed in hours.

The slopes are very similar, indicating that the basic physical phenomenology is the same. The error associated with the data is due to the variability of the thickness in the films. In samples treated with BCP there is a maximum deviation of  $4 \mu\text{m}$ , while in anodized samples this decreases on average to  $2 \mu\text{m}$ .

### Annealing Time

The heat treatments in the presence and absence of tin vapor are essential to control the stoichiometry along the film. In process P2 (Fig. 7 A) Sn remains adhered to the surface due to the surface dipping step. The thermal treatments in the continuous presence of steam involve difficulty in eliminating the macroscopic drops but a stoichiometry of phase A15 of 24-25% is achieved. All the processes, including P2, are described in Fig. 3. A non-uniform Sn layer with an average thickness of 500 nm is present on 52% of the surface. The prolonged heat treatments in the absence of steam lead to minimizing the macroscopic drops, however the stoichiometry of phase A15 decreases.

The sample relative to the process P3 is shown in Fig. 7 (B). This annealing without Sn steam provides a tin concentration lower than 23% in the A15 phase (from EDS and XRD analysis). A non-uniform Sn layer with an average thickness of less than 500 nm is present on the surface. Given the high temperature of the annealing step in the absence of steam, which continues for a long time, there is a degassing of the inconel chamber which promote the formation of a layer rich in Cr (layer of thickness below 500 nm and composition greater than 30%). This contamination is not present in the surface areas covered by residual Sn.

In the “hybrid” process P5 (Fig. 3) the annealing sequence, with Sn steam and after without, is used to first have a slow evaporation of the Sn while maintaining a correct stoichiometry, and consequently, to eliminate the residual tin on the surface and favour sintering. The XRD and EDS characterizations relating to the sample shown in the micrograph in Fig. 7 (C), confirm a concentration of 24-25%. The measurement of the critical temperature ( $T_c$ ) of this sample, carried out at the INFN National Laboratories of Frascati, allows to estimate the stoichiometry at 24% ( $T_c$  13.5 K) as described by Godeke [5]. The macroscopic drops decreased, and the residual surface layer became the 94% of  $\text{Nb}_6\text{Sn}_5$  phase coverage.

The pre-treatment of the substrate plays an important role, in fact in the same process the hybrid heat treatment involves the presence of only phase A15 at 24-25% as shown in Fig. 7 (D) coverage 96% (process P1 sample C2). The Cr contamination in these samples is 40%, this increment is due to the fact that the residual Sn is no longer present when the substrate is initially anodized.

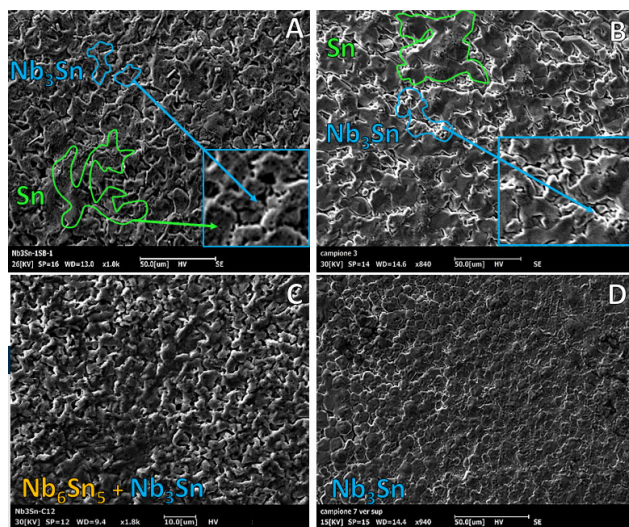


Figure 7: SEM micrographs of samples treated only with BCP and subjected to heat treatments in the presence of steam (A), in the absence of steam (B), hybrid process (C) and influence of the hybrid process with substrate anodization.

### Nb<sub>3</sub>Sn Planar Target

Five targets were synthesized, 4 anodized (T2) and 1 without (T1) with the process P5 (Fig. 3).

The EDS mapping of the target section without anodizing is shown in Fig. 8 (A) process P5 sample T1 (Fig. 3). The Sn average stoichiometry along the film was 26.5%. The qualitative diffractometric analysis operating in goniometric scanning, confirms the presence of a low fraction of the Nb<sub>6</sub>Sn<sub>5</sub> phase. Moreover, no Cr-containing phases are observed. The Cr contamination is only superficial. The Nb<sub>3</sub>Sn film thickness is 28  $\mu$ m in accordance with the expected value within the error.

In Fig. 8 (B) relative to the anodized sample (T2), a surface contamination of Cr greater than 40% is observed. At the diffractometer, no Cr-containing phases are present long the bulk of the film. The average stoichiometry of the film is 26 % and the average thickness is 27  $\mu$ m in accordance with the predictions within the error.

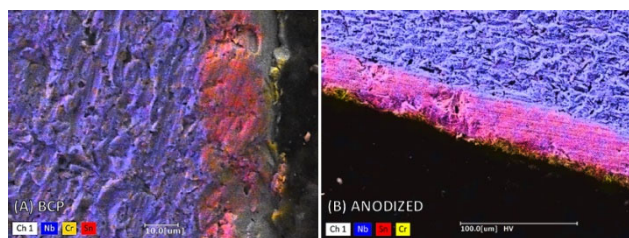


Figure 8: SEM micrographs with EDS mapping of the targets treated with BCP (A) and with the subsequent anodization (B).

### Nb<sub>3</sub>Sn DC Magnetron Sputtering

The Table 1 shows the sputtering process parameters and the target used for Nb<sub>3</sub>Sn on quartz deposition. Only anodized targets synthesized with the optimized process is used.

Table 1: Sputtering Parameters and Processes

Working pressure (Ar)	Deposition time and current	Deposition temperature
<b>Process 1</b>		
1*10 <sup>-2</sup> mbar	26 min 0.1A	750°C
6*10 <sup>-3</sup> mbar	2 h 0.1A	
<b>Process 2</b>		
5*10 <sup>-3</sup> mbar	30 min 0.1A	750°C, more 15 min after process

The aim is the deposition of at least 1  $\mu$ m of Nb<sub>3</sub>Sn on quartz with a Nb<sub>3</sub>Sn thick film of 28  $\mu$ m made via LTD. The post-process annealing in process 2 (Table 1) is used to enhance the correct phase. The target used underwent a total erosion of 21  $\mu$ m on the average 28  $\mu$ m available.

The micrograph (A) in Fig. 9 shows the initial morphology of the target used for deposition. In (B) it is possible to observe the rail track after the sputtering process. From the compositional analysis, only the presence of Nb is highlighted along the trace; preferential Sn sputtering is evident. The XRD pattern show a stoichiometry of 24.5-25% for A15 phase and a small presence of Nb<sub>6</sub>Sn<sub>5</sub> spurious phase. The EDS show a global average of Sn 28%.

In the micrograph (C) in Fig. 9 the crystallites of Nb<sub>3</sub>Sn deposit film of 1.2  $\mu$ m thickness (deposition rate 40 nm/min) show Sn 25-26% with a grains average size of 250 nm; there are clusters of Nb with a size greater than 400 nm in localized areas. The EDS characterization provides a global stoichiometry with Sn 20% confirming the presence of localized Nb. The EDS map of the deposited film is presented in the micrograph (D). The XRD analysis of the sputtered film in Fig. 10 show the A15 phase and the spurious phase as the initial target film (Fig. 11). The extrapolated stoichiometry is Sn 24% with a corresponding extrapolated critical temperature of 13.5 K [5]. The presence of chromium in the deposited film is not detected, probably due to the resolution limit of the EDS instrumentation, the absence of phases containing Cr is also confirmed by the diffractometric analysis.

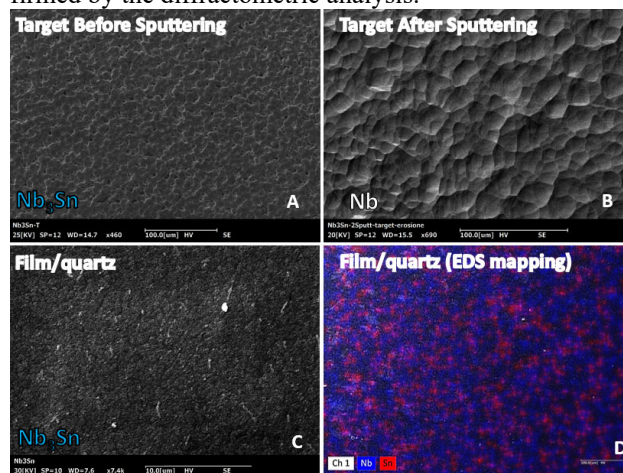


Figure 9: SEM micrographs of the targets before sputtering process (A) and rail track after the process (B). Nb<sub>3</sub>Sn deposition on quartz (C) and EDS mapping (D).

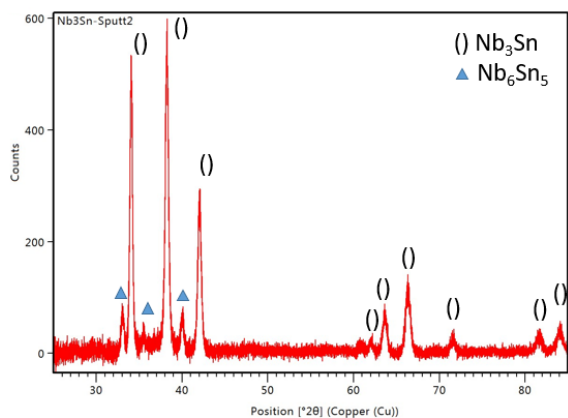


Figure 10: XRD of  $Nb_3Sn$  film on quartz.

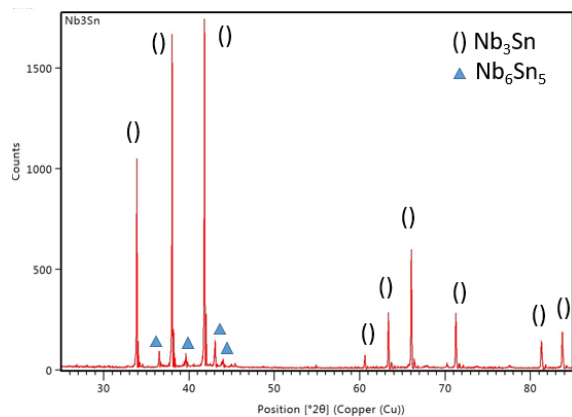


Figure 11: XRD the target (anodized) before sputtering.

## CONCLUSIONS

It has been demonstrated that the controlled nucleation process is fundamental for an efficient success of the process in terms of film quality. The macroscopic tin droplets are considerably reduced, and spurious phases are minimized in the A15 allowing a better maintenance of the ideal stoichiometry of 25% of Sn.

The dipping time is the predominant factor in increasing the film thickness. The relationships found for Fick's law allow to estimate the thickness as a function of the immersion time. The 5-hours processes allow to obtain 28  $\mu\text{m}$  sufficient for the deposition of 1  $\mu\text{m}$  of  $Nb_3Sn$  via DCMS sputtering.

The "hybrid" heat treatment is essential to obtain a correct stoichiometry and minimization of the spurious

phases. This type of process with the use of anodized substrates will be used as a standard for the manufacture of subsequent targets.

The single-use thick film planar targets of  $Nb_3Sn$  via LTD technique for DC magnetron sputtering depositions were obtained and successfully used.

The characterization of the sputtered film on quartz from  $Nb_3Sn$  target via LTD confirms the A15 phase in the deposit. The coating has characteristics and stoichiometry comparable to the starting target thick film of Sn 24-25%.

To eliminate chromium contamination in the LTD process, a niobium screen will be inserted inside the chamber and the deposition system will be modified with a shutter to perform a pre-sputtering with which to clean the target from unreacted Sn or Cr.

In the near future the LTD optimized process will be implemented on cylindrical geometry cathodes and a systematic study on sputtering deposition parameters will be performed.

## ACKNOWLEDGEMENTS

Work supported by the INFN CSNV experiment TEFEN, agreement N.KE2722/BE/FCC.

This project has received funding from the European Union's Horizon 2020 Research and Innovation programme under GA No 101004730 I.FAST project.

## REFERENCES

- [1] E. A. Ilyina *et al.*, "Development of sputtered  $Nb_3Sn$  films on copper substrates for superconducting radiofrequency applications", *Supercond. Sci. Technol.*, vol. 32, no. 3, p. 035002, 2019. <https://doi.org/10.1088/1361-6668/aaf61f>
- [2] S. M. Deambrosis *et al.*, "A15 superconductors: An alternative to niobium for RF cavities", *Physica C*, vol. 441, iss. 1-2, pp. 108-113, 2006. <https://doi.org/10.1016/j.physc.2006.03.047>
- [3] M. Zanierato, "Studio e sviluppo delle tecniche di deposizione di film sottili di  $Nb_3Sn$  per applicazioni in cavità risonanti", Master's Degree Thesis, Department of Chemical Science, University of Padua, Italy, 2020.
- [4] M. Zanierato *et al.*, "Optimization of the Liquid Diffusion Process to produce  $Nb_3Sn$  Films for Superconducting Radio Frequency Applications", INFN-LNL, Padua, Italy, 2020.
- [5] A. Godeke, "A review of the properties of  $Nb_3Sn$  and their variation with A15 composition, morphology and strain state", *Supercond. Sci. Technol.*, vol. 19, no. 8, p. R68, 2006. <https://doi.org/10.1088/0953-2048/19/8/R02>